SPATIALLY-LOCALIZED SCAFFOLD PROTEINS MAY FACILITATE TO TRANSMIT LONG-RANGE SIGNALS[*]

Dedicated to Professor James Glimm on the occasion of his 75th birthday

Xinfeng Liu

Department of Mathematics, University of South Carolina, Columbia, SC 29208, USA
E-mail: xfliu77@gmail.com

Qing Nie

Department of Mathematics, Center for Mathematical and Computational Biology,
University of California, Irvine, CA 92697, USA
E-mail: qnie@math.uci.edu

Abstract Scaffold proteins play an important role in the promotion of signal transmission and specificity during cell signaling. In cells, signaling proteins that make up a pathway are often physically orgnaized into complexes by scaffold proteins [1]. Previous work [2] has shown that spatial localization of scaffold can enhance signaling locally while simultaneously suppressing signaling at a distance, and the membrane confinement of scaffold proteins may result in a precipitous spatial gradient of the active product protein, high close to the membrane and low within the cell. However, cell-fate decisions critically depend on the temporal pattern of product protein close to the nucleus. In this paper, when phosphorylation signals cannot be transfered by diffusion only, two mechanisms have been proposed for long-range signaling within cells: multiple locations of scaffold proteins and dynamical movement of scaffold proteins. Thus, here we have unveiled how the spatial propagation of the phosphorylated product protein within a cell depends on the spatially and temporal localized scaffold proteins. A class of novel and fast numerical methods for solving stiff reaction diffusion equations with complex domains is briefly introduced.

Key words scaffold proteins; signal pathway; reaction-diffusion equations

2000 MR Subject Classification 92B99; 65M06

1 Introduction

Cells have to respond to changes in the environment and/or to the external stimuli. This is accomplished by signal transduction pathways which sense the signal, transduce it, and induce

necessary changes in the cell, such as in gene expression. Scaffold proteins are thought to play a key role during this process [1, 3–7]. Well known examples of scaffold proteins include yeast Ste5 and mammalian JIP proteins, which bind to all the kinases in a particular mitogen-activated protein kinase (MAPK) cascade.

Scaffold usually dynamically binds to two or more consecutively-acting components of a signaling cascade, and it links signaling molecules into linear pathways by physically assembling them into complexes. Experimental work suggests that scaffolds may promote signal transmission by tethering consecutively acting kinases near each other [8, 9]. However, it has also been experimentally observed that some scaffold inhibit signaling when overexperssed [10–12]. Supporting these observations, computations of non-spatial models have demonstrated that scaffold proteins may either enhance or suppress signaling, depending on the concentration of scaffold. In [2], a model of generic, spatially localized scaffold protein was developed for one spatial dimension, and the model indicated that a scaffold protein could boost signaling locally (in and near the region where it was localized) while simultaneously suppressing signaling at a distance. Owing to the confinement of scaffold proteins to the cell membrane and the dephosphorylation during diffusion through the cytoplasm, the phosphorylated level of active product proteins may become low near the nucleus. Given measured values of localized scaffold proteins and diffusivity, it was demonstrated that the active product protein would drop precipitously, becoming negligible at the distance of several microns from the plasma membrane [13, 14].

In view of this rapid decline in the active phosphorylation product protein spreading solely by diffusion, alternative mechanisms to relay stimuli from the plasma membrane to distant targets have been proposed, such as (i) trafficking of phosphorylated kinases within endocytic vesicles or non-vesicular signaling complexes by molecular motores [15–18] and (ii) phosphoprotein waves propagating from the membrane over long distances, especailly in large cells, such as starfish oocytes or Xenopus oocytes [19, 20].

In the present paper, when phosphorylation signals cannot be transfered by diffusion only, we have proposed the following two alternative mechanisms for long-range signaling within cells: multiple locations and dynamical movement of scaffold proteins. Through a generic mathematical model to describe a spatially localized scaffold and freely diffusing products and reactants, our numerical simulations exhibit that the distribution of scaffold into multiple local regions might enhance signaling near nucleus, depending on the locations of scaffold proteins. Moreover, the simulations suggest that the movement of scaffold from the cell nucleus to a particular location near cell membrane might increase the rate of signal transmission during this process. Thus, here we have unveiled how the spatial propagation of the phosphorylated product protein within a cell depends on the spatially localized scaffold proteins by various mechanisms.

A system of stiff reaction diffusion equations has been applied to model the protein reactions and diffusible reactants. For reaction-diffusion equations, the authors in [21] have developed a class of implicit integration factor (IIF) method that are computationally much cheaper than fully implicit schemes and can be unconditional stable or have generous stability conditions. In IIF, the diffusion term is treated exactly such that the stability constraint due to spatial discretization for diffusion is removed while the reaction term is treated implicitly to handle the stiffness of reaction terms. As a result, the scheme is semi-implicit and linearly

unconditional stable for its second order scheme and has large stability regions for the high order scheme. In terms of computational cost, IIF has the same order of computational complexity as explicit integration factor methods (or exponential time difference methods) because the explicit treatment of diffusion (a global term) is decoupled from the implicit treatment of reaction terms.

To efficiently store and compute the exponential matrices in IIF for two and three dimensional systems, later we introduced a class of compact implicit integration factor (cIIF) method [22] that has the same stability properties as the original IIF [21] but with significant improvement on storages and computational savings for high spatial dimensions.

All the systems discussed in [22] are with Cartesian coordinates, but for complex domains, curvilinear coordinates are simpler to use with various real applications. However, it is very challenging to write the diffusion matrices for a complex domain with curvilinear coordinates. Curvilinear coordinates, converting the standard coordinate system to a coordinate system in which the coordinate lines are curved, are much simpler to use depending on the applications, such as the shape of cells and embryos. The conversion of Cartesian coordinates is based on some transformation, which is required to be locally invertible (one-to-one map) at each point. Polar coordinates for R^2 and spherical or cylinder coordinates for R^3 are well known examples of curvilinear systems. For instance in the systems cell biology, the cells are usually considered with spherical or circular symmetry, which are easier to solve in spherical or polar coordinates. In order to efficiently handle the complex domains with circular or spherical symmetry, recently we have extended the compact implicit integration factor method to the system with polar/spherical coordinates, which is similar to the method in a cartesian coordinate system [22].

The remainder of the paper is organized as follows. In Section 2 we discuss a mathematical model to describe the protein reactions with scaffold interactions. The numerical scheme to solve this model is briefly introduced in Section 3, and in Section 4 the numerical simulation results and discussions are presented, and the conclusion is reported in Section 5.

2   Mathematical Models

In this paper, we assumed that the cell consists of two compartments, which are assumed to be biophysically and biochemically identical. The only difference between two apartments is that one apartment contains the scaffold protein, and the other does not. The scaffold-containing compartment was placed in the region near the membrane, or moving to membrane during signaling. The scaffold is stuck in its compartment and does not diffuse. In contrast, other reactants without scaffold binding diffuse freely throughout the cell.

The model contains a scaffold protein (S), which can bind to two other proteins (A and B). In the absence of the scaffold protein, A and B can bind directly to each other. In the presence of the scaffold protein S, first A binds to S, forming AS. Next B binds to AS forming ASB. Moreoever, both AB and ABS can be dissociated into a phosphorylated form B^p. Finally, A and B bind to each other on the scaffold. The symmetrical path, where B binds to the scaffold before A, is also available. Denote [ ] as the concentration of the proteins, the mass action

equations with diffusion take the form,

$$\frac{\mathrm{d}[S]}{\mathrm{d}t} = -j_{\mathrm{on}}([A][S] + [B][S]) + j_{\mathrm{off}}([AS] + [BS]) + j_{\mathrm{p}}[ABS],$$

$$\frac{\mathrm{d}[AS]}{\mathrm{d}t} = j_{\mathrm{on}}([A][S] - [AS][B]) - j_{\mathrm{off}}([AS] - [ABS]),$$

$$\frac{\mathrm{d}[BS]}{\mathrm{d}t} = j_{\mathrm{on}}([B][S] - [BS][A]) - j_{\mathrm{off}}([BS] - [ABS]),$$

$$\frac{\mathrm{d}[ABS]}{\mathrm{d}t} = j_{\mathrm{on}}([AS][B] + [BS][A]) - (2j_{\mathrm{off}} + j_p)[ABS],$$

$$\frac{\mathrm{d}[A]}{\mathrm{d}t} = D\Delta[A] - k_{\mathrm{on}}[A][B] + k_{\mathrm{off}}[AB] - j_{\mathrm{on}}([A][S] + [BS][A]) \quad\quad (1)$$
$$+ j_{\mathrm{off}}([AS] + [ABS]) + k_p[AB] + j_p[ABS],$$

$$\frac{\mathrm{d}[B]}{\mathrm{d}t} = D\Delta[B] - k_{\mathrm{on}}[A][B] + k_{\mathrm{off}}[AB] - j_{\mathrm{on}}([B][S] + [AS][B])$$
$$+ j_{\mathrm{off}}([BS] + [ABS]) + d_1[B^p],$$

$$\frac{\mathrm{d}[AB]}{\mathrm{d}t} = D\Delta[AB] + k_{\mathrm{on}}[A][B] - k_{\mathrm{off}}[AB] - k_p[AB]$$

$$\frac{D[B^p]}{\mathrm{d}t} = D\Delta[B^p] + j_p[ABS] - d_1[B^p] + k_p[AB].$$

In the system (1), the set of parameters are specified as the following, $D = 10^{-7}\mathrm{cm}^2/\mathrm{s}$ for a high value of diffusion constant and $D = 10^{-8}\mathrm{cm}^2/\mathrm{s}$ for a low value of diffusion constant; $k_{\mathrm{on}} = 1(\mu\mathrm{M\ s})^{-1}, k_{\mathrm{off}} = 3(\mathrm{s})^{-1}, k_p = 0.1(\mathrm{s})^{-1}, d_1 = 1(\mathrm{s})^{-1}$ are the on and off rates for the off-scaffold reactions, $j_{\mathrm{on}} = 100(\mu\mathrm{M\ s})^{-1}, j_{\mathrm{off}} = 0.5(\mathrm{s})^{-1}, j_{\mathrm{con}} = 1(\mathrm{s})^{-1}, j_p = 1(\mathrm{s})^{-1}$ are the rate constants for the on-scaffold reactions. The units for the time and length are second and centimeter respectively. This set of parameters is particularily selected based on the reason that the scaffold binding rate is more significant than off-scaffold binding ones, such that our study of spatial and temporal dynamics of scaffold would be more prominent [2].

3   Numerical Methods

The general reaction diffusion system in polar coordinates with no-flux boundary conditions takes the following form

$$\begin{cases} \dfrac{\partial \mathbf{u}}{\partial t} = D\left(\dfrac{\partial^2 \mathbf{u}}{\partial r^2} + \dfrac{1}{r^2}\dfrac{\partial^2 \mathbf{u}}{\partial \theta^2} + \dfrac{1}{r}\dfrac{\partial \mathbf{u}}{\partial r}\right) + \mathbf{F}(\mathbf{u}), \quad (r,\theta) \in \Omega = \{a < r < b, c < \theta < d\}; \\ \dfrac{\partial \mathbf{u}}{\partial r}(a,\theta) = \dfrac{\partial \mathbf{u}}{\partial r}(b,\theta) = \dfrac{\partial \mathbf{u}}{\partial \theta}(r,c) = \dfrac{\partial \mathbf{u}}{\partial \theta}(r,d) = 0. \end{cases} \quad (2)$$

After discretizing the spatial domain by a rectangular mesh: $(r_i, \theta_j) = (a + (i-1)h_r, c + (j-1)h_\theta)$ where $h_r = (b-a)/(N-1)$, $h_\theta = (d-c)/(M-1)$, $r_i = (i-1)h_r$ and $1 \le i \le N$ and $1 \le j \le M$, we use the second order central difference discretization for the diffusion terms:

$$\frac{\mathrm{d}u_{i,j}}{\mathrm{d}t} = D\left(\frac{u_{i+1,j} - 2u_{i,j} + u_{i-1,j}}{h_r^2} + \frac{u_{i,j+1} - 2u_{i,j} + u_{i,j-1}}{r_i^2 h_\theta^2} + \frac{u_{i+1,j} - u_{i-1,j}}{2r_i h_r}\right) + \mathbf{F}(u_{i,j}). \quad (3)$$

To express (2) in a compact form, we define the matrix $\mathbf{U}$ for the discretized solutions:

$$\mathbf{U} = \begin{pmatrix} u_{1,1} & u_{1,2} & \cdots & u_{1,M} & u_{1,M} \\ u_{2,1} & u_{2,2} & \cdots & u_{2,M} & u_{2,M} \\ \vdots & \vdots & \vdots & \vdots & \vdots \\ u_{N,1} & u_{N,2} & \cdots & u_{N,M} & u_{N,M} \end{pmatrix}_{N \times M},$$

and

$$\mathbf{G}_{P \times P} = \begin{pmatrix} -2 & 2 & 0 & 0 & \cdots & 0 \\ 1 & -2 & 1 & 0 & \cdots & 0 \\ 0 & 1 & -2 & 1 & \cdots & 0 \\ & & \ddots & \ddots & \ddots & \\ 0 & 0 & \cdots & 1 & -2 & 1 \\ 0 & 0 & \cdots & 0 & 2 & -2 \end{pmatrix}_{P \times P},$$

$$\mathbf{E}_{P \times P} = \begin{pmatrix} 0 & 0 & 0 & 0 & \cdots & 0 \\ -1/r_2 & 0 & 1/r_2 & 0 & \cdots & 0 \\ 0 & -1/r_3 & 0 & 1/r_3 & & 0 \\ & & \ddots & \ddots & \ddots & \\ 0 & \cdots & 0 & -1/r_{P-1} & 0 & 1/r_{P-1} \\ 0 & 0 & 0 & \cdots & 0 & 0 \end{pmatrix}_{P \times P},$$

$$\mathbf{F}_{P \times P} = \begin{pmatrix} 1/r_1^2 & 0 & 0 & 0 & \cdots & 0 \\ 0 & 1/r_2^2 & 0 & 0 & \cdots & 0 \\ 0 & 0 & 1/r_3^2 & 0 & \cdots & 0 \\ & & \ddots & \ddots & \ddots & \\ 0 & 0 & \cdots & 0 & 1/r_{P-1}^2 & 0 \\ 0 & 0 & 0 & \cdots & 0 & 1/r_P^2 \end{pmatrix}_{P \times P}.$$

After defining $\mathbf{A}_1 = \frac{D}{h_r^2}\mathbf{G}_{N \times N}, \mathbf{B} = \frac{D}{h_\theta^2}\mathbf{G}_{M \times M}, \mathbf{A}_2 = \frac{D}{2h_r}\mathbf{E}_{N \times N}, \mathbf{C} = \mathbf{F}_{N \times N}$, and $\mathbf{A} = \mathbf{A}_1 + \mathbf{A}_2$, we re-write the semi-discretized form (3) as

$$\frac{\mathrm{d}\mathbf{U}}{\mathrm{d}t} = \mathbf{A}\mathbf{U} + \mathbf{C}\mathbf{U}\mathbf{B} + \mathcal{F}(\mathbf{U}). \tag{4}$$

Assume that matrix B is diagonalizable with $\mathbf{B} = \mathbf{P}\tilde{\mathbf{D}}\mathbf{P}^{-1}$. Both matrices $\mathbf{C}$ and $\tilde{\mathbf{D}}$ are diagonal, with the i-th and j-th diagonal elements for $\mathbf{C}$ and $\tilde{\mathbf{D}}$ being c_i and d_j, respectively. And define

$$\tilde{\mathbf{C}} = (\tilde{c}_{ij}) = (c_i d_j),$$

where $i = 1, 2, \cdots, N, j = 1, 2, \cdots, M$, and an operation '$(e^*)$' is defined by taking exponentials element by element,

$$(e^*)^{\tilde{\mathbf{C}}} = (e^{\tilde{c}_{ij}}),$$

Define another operator '$\odot$' for two matrices through element by element multiplication:

$$(\mathbf{H} \odot \mathbf{L})_{i,j} = (h_{ij}l_{ij}),$$

where $\mathbf{H} = (h_{ij}), \mathbf{L} = (l_{ij})$.

The details of analysis and derivation on numerical methods for solving (4) will be published in a separate publication. Here we use a second order numerical scheme, which has the following time stepping algorithm,

$$\mathbf{U}_{n+1} = e^{\mathbf{A}\Delta t} \left(\mathbf{U}_n + \frac{\Delta t}{2}\mathcal{F}(\mathbf{U}_n) \right) \tilde{\mathbf{B}} + \frac{\Delta t}{2}\mathcal{F}(\mathbf{U}_{n+1}), \tag{5}$$

where $\tilde{\mathbf{B}} = \mathbf{P} \odot (e^*)^{\tilde{\mathbf{C}}\Delta t}\mathbf{P}^{-1}$.

To test the accuracy and efficiency of the cIIF scheme (5) in polar coordinate, we study the following system of the polar coordinate:

$$\begin{cases} \dfrac{\partial \mathbf{u}}{\partial t} = 0.1 \left(\dfrac{\partial^2 \mathbf{u}}{\partial r^2} + \dfrac{1}{r^2}\dfrac{\partial^2 \mathbf{u}}{\partial \theta^2} + \dfrac{1}{r}\dfrac{\partial \mathbf{u}}{\partial r} \right) + 0.2\mathbf{u}, \quad (x,y) \in \Omega = \{5 < r < 10, 0 < \theta < \pi\}; \\ \mathbf{u}(r,\theta) \mid_{r=5} = e^{0.1t}\cos(5\cos\theta)\cos(5\sin\theta); \\ \mathbf{u}(r,\theta) \mid_{r=10} = e^{0.1t}\cos(10\cos\theta)\cos(10\sin\theta); \\ \mathbf{u}(r,\theta) \mid_{\theta=0} = e^{0.1t}\cos(r); \mathbf{u}(r,\theta) \mid_{\theta=\pi} = e^{0.1t}\cos(r). \end{cases} \tag{6}$$

This system (6) has the exact solution $\mathbf{u}(r,\theta) = e^{0.1t}\cos(r\cos\theta)\cos(r\sin\theta)$.

The error is calculated using the maximal error between the numerical solution and the exact solution. The numerical calculation is carried up to time $t = 2$, and the number of grid points for the r and θ is set equal for convenience of comparison. The time step size is set as $\Delta t = 0.5h_r$ for the sake of testing accuracy. As seen in Table 1, the calculation using the scheme (5) is of order two and the time step is not constrained like typical explicit temporal schemes, and the stability property and computational cost of the scheme (5) is similar to the standard cIIF2 [22].

Table 1   Error, order of accuracy, and CPU time for cIIF2 for a two-dimensional case (6). The unit for CPU is second.

$N \times N$	L^∞ error	order	CPU
40×40	4.58×10^{-3}	—	0.23
80×80	1.23×10^{-3}	1.90	0.52
160×160	3.1×10^{-4}	1.99	2.41
320×320	8.23×10^{-5}	1.91	64.24

4   Results

In this section, we focus on the two dimensional simulation, in which the system (1) holds in the cell, which is modeled as a disk with a radius 10cm: $\Omega = \{x^2 + y^2 \leq 100\text{cm}^2\}$. No-flux boundary conditions is superimposed for the diffusible components A, B, AB, B^p. The

starting concentrations of A and B are set at 1μM, uniformly distributed throughout the cell. The starting total concentration of S is set at $150\pi\mu$M or specified otherwise, and equally distributed within one or multiple local regions. All other reactants $AB, B^p, AS, BS,$ and ABS are initially set equal to 0 everywhere. The accuracy and convergence of numerical solutions were examined by the predicted total amount steady state of A present in all complexes. If the numerical solution is 100% accurate, this number should add up to the initial total amount. In all our numerical simulations, the calculated percentage error for this number is within 5%.

4.1   Scaffold with multiple locations might create long-range signaling

Scaffold proteins are often confined to a or several locations in the cell, or move to that region during signaling. Yeast Ste5 localizes first to the cell nucleus, and then move to the region of the cell closest to the source of the signal [23, 24], and yeast Spa2 localizes to regions of polarized growth [25]. Yet other scaffolds are localized elsewhere in the cell when active. A model [2] indicated that a confined scaffold protein in one particular domain could boost signaling locally (in and near the region where it was localized) while simultaneously suppressing signaling at a distance.

In this subsection, the effect of scaffold proteins with multiple locations in two dimensions is explored with a mathematical model described in Section 2. In our numerical simulations, scaffold proteins are equally distribued into several local regions with the initial total amount set to a value of $150\pi\mu$M. Seven scenarios are considered in this context, in which scaffold proteins are initially and equally distributed into one, two, three or four local regimes. For the the scaffold proteins in two, three or four locations, both symmetric and asymmetric cases were presented. Asymmetric cases mean that the scaffold are equally distributed in multiple regions which are symmetric only from left to right, and located in the upper half cell (Fig.1). Symmetric cases mean that the scaffold proteins are equally distributed in multiple regions which are symmetric in two directions, from left to right and bottom to top (Fig.2). The product protein B^p for four cases in the cell are reported: (A) nucleus (center); (B) middle from the cell nucleus (center) to cell membrane (north pole); (C) cell membrane (north pole); (D) total B^p throughout the whole cell. A two dimensional contour plot is also presented.

Multiple locations of scaffold proteins might generate long-range signaling within cells   The spatially localized scaffold in a particular domain within a cell could lead to a steep gradient of product protein B^p. Given measured protein diffusivity and scaffold activity, signal propagation by diffusion would result in a steep decline of product activity and low product levels near the nucleus [2]. The system with multiple locations of scaffold proteins for asymmetric cases could generate a novel type of phosproptein wave that propagates from the cell surface (membrane) deep into the cell interior (nucleus), and thus enhance the propagation span of the product protein B^p (Fig. 1, 2). Distribution of the scaffold into more regions leads to stronger signals near the cell nucleus. For the case of symmetric multiple locations of scaffold proteins, the system exhibits a similar trend as those with asymmetric cases, but with a lower effect (Fig. 1, 2).

Multiple locations of scaffold proteins can enhance total product formation The total amount of product protein B^p, which are summed across the entire cell, are studied as well for different multiple domains, with an initial total scaffold protein set equal to a constant for all cases. For the scenario with asymmetric distribution of scaffold (Fig. 1), it shows that

localization of the scaffold with more regions leads to a larger value of total product poteins B^p. A similar trend is observed for symmetrical cases (Fig. 2). Hence in general, localization of the scaffold produces less total product than those with the same amount of total scaffold being delocalized. In summary, our numerical simulations show that several multiple locations of the scaffold can interact with each other during signaling transduction, and increase the level of activity of the product protein B^p throughout the whole cell.
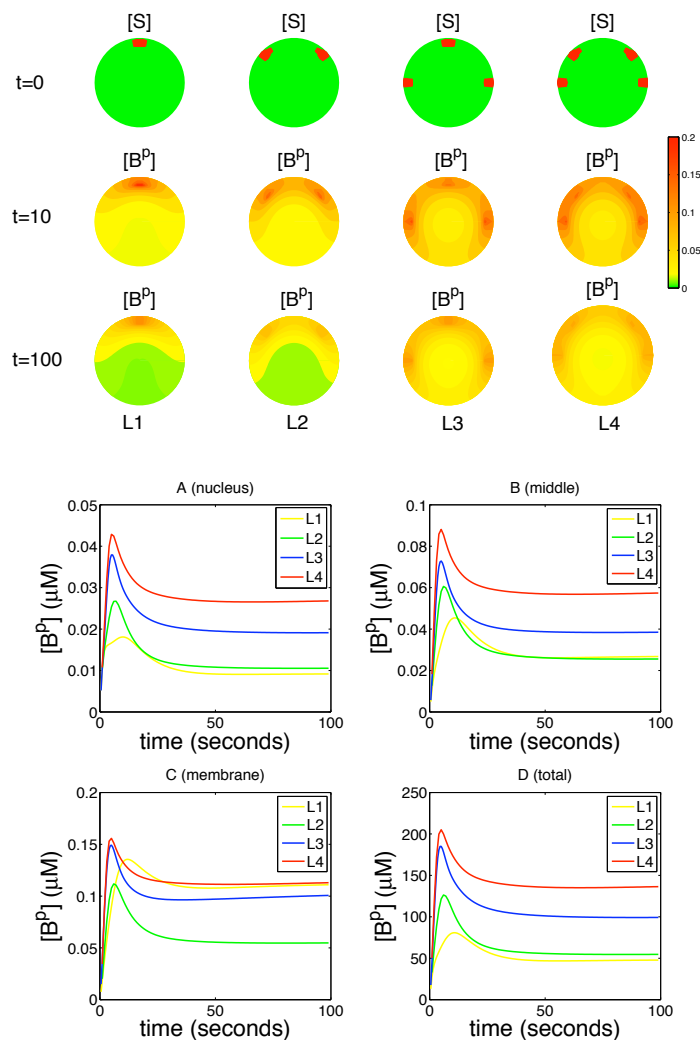
Fig.1   Concentration of B^p with multiple asymmetric scaffold locations. L1: Scaffold localized at one region; L2: Scaffold localized at two regions; L3: Scaffold localized at three regions; L4: Scaffold localized at four regions. (A) B^p at the nucleus; (B) B^p in the middle from north pole to nucleus; (C) B^p at the north pole; (D) total B^p.

4.2   Moving scaffold during cell signaling may generate propagation wave

Scaffold proteins often move to the local region instead of confining to a particular location in the cell during signaling. Recent experiment demonstrates that scaffold protein Ste5 in the MAPK kinase pathway will move from the interior of cell to the cell membrane in about six

seconds after the cell surface receptor is activated [26]. The dynamical movement of scaffold proteins might generate the propagation wave through cell signaling pathways. Based on the experimental observation [26], we build a mathematical model in which the scaffold along with its complex move from the interior of the cell close to its nucleus to cell membrane with a linear velocity (Fig. 3). The numerical experiments are set up as the following: The scaffold proteins are initially localized within a small disk with a radius of 1cm, and the distance of its center to the cell nucleus is 3cm. When the signal pathway is activated, the scaffold along with its complex start moving to the cell membrane in a straight line with a speed of 1cm/s, and after about 6 seconds the scaffolds stop at a local region near the cell membrane and stay there for the rest of signal transduction.
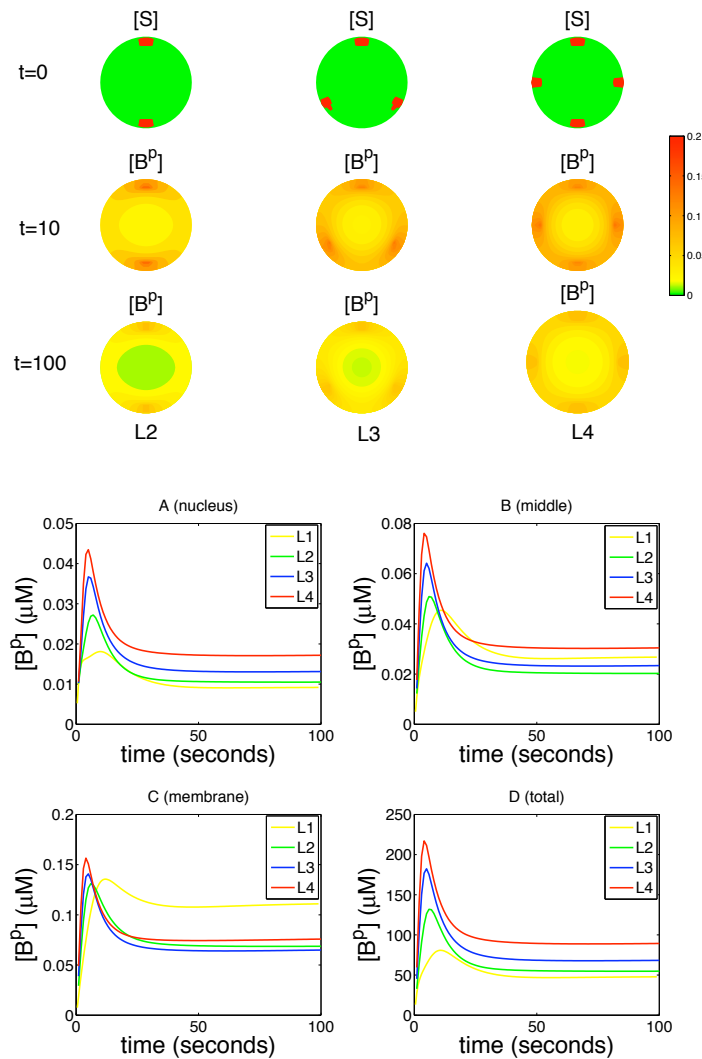
Fig.2   Concentration of B^p with multiple symmetric scaffold locations. L1: Scaffold localized at one region; L2: Scaffold localized at two regions; L3: Scaffold localized at three regions; L4: Scaffold localized at four regions. (A) B^p at the nucleus; (B) B^p in the middle from north pole to nucleus; (C) B^p at the north pole; (D) total B^p.
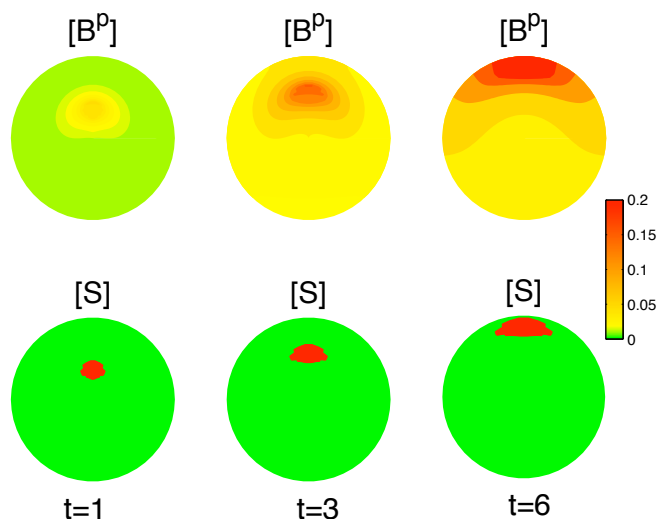
Fig.3   Concentration of B^p and S at different times with moving scaffold
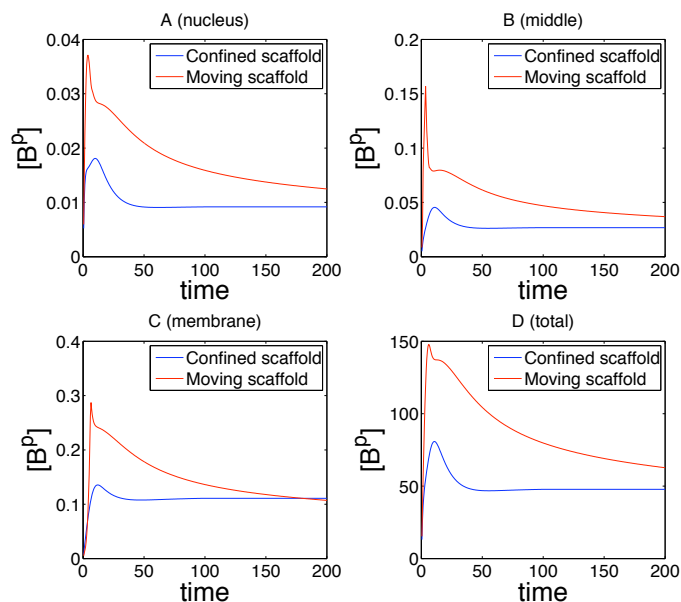
Fig.4 B^p v.s. time for the moving scaffold. (A) B^p at the nucleus; (B) B^p in the middle from north pole to nucleus; (C) B^p at the north pole; (D) total B^p

     The protein reactions with moving scaffold are still modeled as in Eq.(1), with the scaffold protein S and its complex AS, BS, ABS translocating from a local region near the cell nucleus to the cell membrane within 6 seconds. As with the same discussion in section Section 4.1, the phosphorylated product protein B^p is measured for four scenarios (Fig. 4): (A) cell nucleus (center); (B) middle of cell nucleus (center) to the membrane (north pole); (C): cell membrane (north pole); (D) total B^p throughout the whole cell. Compared to the system with the

confined scaffold, the system with dynamical moving scaffold delays the signal propagation while increasing the level of the active B^p fraction at the nucleus (Fig. 4). Moreover, the system with moving scaffold needs longer time to reach steady state, and the maximum amplitude of the signal B^p is much greater than that of the system with stationary scaffold proteins. In summary, the numerical simulations exhibit that dynamical moving scaffold might enhance the signal propagation span and thus increase the level of the total product protein B^p.
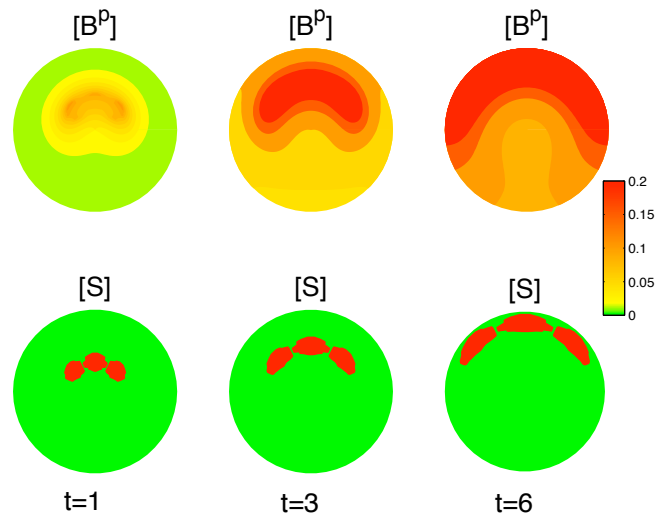
Fig.5   Concentration of B^p and S at different times with moving multiple scaffold
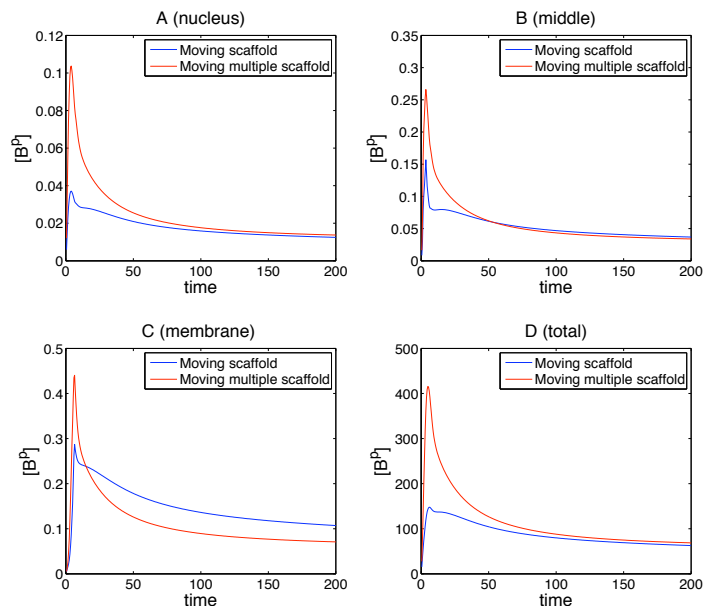
Fig.6 B^p v.s. time for the moving scaffold, compared to the system with moving scaffold which is split into three parts. (A) B^p at the nucleus; (B) B^p in the middle from north pole to nucleus; (C) B^p at the north pole; (D) total B^p.

Next we consider the following scenario: the scaffold proteins move from the interior of the cell near nucleus to cell membrane, and split into several parts during this translocation. One simple simulation model is applied to describe this phenomena. Initially scaffold begins to move from a local region near the nucleus when the receptor is activated. After one second, the scaffold is divided equally into three parts and move to the cell membrane in straight lines with a linear velocity. One part remains the same direction as before, and the other two move in the radial direction symmetrical to the initial direction with an angle of $\pi/4$ (Fig. 5) at a constant speed. Compared to the scenario that one whole piece of scaffold moves to the membrane, the system with the moving scaffold which are split into three parts can increase the maximum amplitude of the signal at the cell nucleus for the early stage, however, both systems reach almost the same steady states at a later time (Fig. 6).

5 Conclusion

Previous computational and theoretical studies of scaffold proteins have assumed a homogeneous distribution or single spatially localized scaffold and their ligands. Here using a mathematical model to describe the protein reactions, we have unveiled the possible outcomes when scaffold proteinis are spatially localized at several multiple locations, and/or are moving from cell nucleus to cell membrane. Through various numerical experiments, we have shown that multiple scaffold localizations allows the protein reaction to interact with each other and thus enhance the transmission of signals to the cell nucleus. The dynamical movement of scaffold proteins from cell nucleus to cell membrane might create a signaling traveling wave, and thus facilitate signal transfer during transduction. The scaffold might shield the signaling pathway, allowing capabilities of feedback loops and interaction with kinase dynamically, and it could dramatically enhance signaling at a long distance. Therefore in this paper we have provided several potential mechanisms in which the signals can travel at a long distance and could be amplified to cell nucleus during the process of transmission. We have also briefly introduced a compact integration factor method for stiff reaction diffusion equations with curvilinear coordinates, in which the stability condition, computational cost and storage are similar to the method in a Cartesian system.

References

[1] Pawson T, Scott J D. Signaling through scaffold, anchoring, and adaptor proteins. Science, 1997, **278**: 2075–2080

[2] Bardwell L, Liu X F, Moore R D, Nie Q. Spatially-localized scaffold proteins may simultaneously boost and suppress signaling. Preprint, 2009

[3] Burack W R, Shaw A S. Signal transduction: hanging on a scaffold. Curr Opin Cell Biol, 2000, **12**: 211–216

[4] Bhattacharyya R P, Remenyi A, Yeh B J, Lim W A. Domians, motifs, and scaffolds: The role of modular interactions in evolution and wiring of cell signaling circuits. Annu Rev Biochem, 2006, **75**: 655–680

[5] Whitmarsh A J, Davis R J. Structural organization of MAP-kinase signaling modules by scaffold proteins in yeast and mammals. Trends Biochem Sci, 1998, **23**: 481–485

[6] Morrison D K, Davis R J. Regulation of MAP Kinase signaling modules by scaffold proteins in mammals. Annu Rev Cell Dev Biol, 2003, **19**: 91–118

[7] Wong W, Scott J D. AKAP signalling complexes: focal points in space and time. Nat Rev Mol Cell Biol, 2004, **5**: 959–970

[8] Park S H, Zarrinpar A, Lim W A. Rewiring MAP kinase pathways using alternative scaffold assembly mechanisms. Science, 2003, **299**: 1061–1064

[9] Harris K, Lamson R E, Nelson B, Hughes T R, Marton M J, Roberts C J, Boone C, Pryciak P M. Role of scaffolds in MAP kinase pathway specificity revealed by custom design of pathway-dedicated signaling proteins. Curr Biol, 2001, **11**: 1815–1824

[10] Dickens M, Rogers J S, Cavanagh J, Raitano A, Xia Z, Halpern J R, Greenberg M E, Sawyers C L, Davis R J. A cytoplasmic inhibitor of the JNK signal transduction pathway. Science, 1997, **277**: 693–696

[11] Cohen L, Henzel W J, Baeuerle P A. IKAP is a scaffold protein of the IkB kinase complex. Nature, 1998, **395**: 292–296

[12] Kortum R L, Lewis R E. The molecular scaffold KSR1 regulates the proliferative and oncogenic potential of cells. Mol Cell Biol, 2004, **24**: 4407–4416

[13] Kholodenko B N. Negative feedback and ultrasensitivity can bring about oscillations in the motigen-activated protein kinase cascades. Eur J Biochem, 2000, **267**: 1583–1588

[14] Maly I V, Wiley H S, Lauffenburger D A. Self-orgnization of polarized cell signaling via autocrine circuits: computational model and analysis. Biophys J, 2004, **86**: 10–22

[15] Howe C L, Mobley W C. Signaling endosome hypothesis: A cellular mechanism for long distance communication. Journal of Neurobiology, 2004, **58**(2): 207–216

[16] Kholodenko B N. MAP kinase cascade signaling and endocytic trafficking: a marriage of convenience? Trends in Cell Biology, 2002, **12**(4): 173–177

[17] Miaczynska M, Pelkmans L, Zerial M. Not just a sink: endosomes in control of signal transduction. Current Opinion in Cell Biology, 2004, **16**(4): 400–406

[18] Perlson E, Hanz S, Ben-Yaakov K, Segal-Ruder Y, Seger R, Fainzilber M. Vimentin-dependent spatial translocation of an activated MAP kinase in injured nerve. Neuron, 2005, **45**(5): 715–726

[19] Kholodenko B N. Four-dimensional organization of protein kinase signaling cascades: the roles of diffusion, endocytosis and molecular motors. Journal of Experimental Biology, 2003, **206**(12): 2073–2082

[20] Slepchenko B M, Terasaki M. Cyclin aggregation and robustness of bio-switching. Molecular Biology of the Cell, 2003, **14**(11): 4695–4706

[21] Zhang Y -T, Nie Q, Zhao R. Efficient semi-implicit schemes for stiff systems. Journal of Computational Physics, 2006, **214**: 521–537

[22] Zhang Y T, Nie Q, Wan F Y M, Liu X F. Integration factor methods for high spatial dimensions. Journal of Computational Physics, 2008, **277**: 5238–5255

[23] Elion E A. The Ste5p scaffold, 2001

[24] van Drogen F, Peter M. MAP kinase dynamics in yeast. Biol Cell, 2001, **93**(1/2): 63–70

[25] van Drogen F, Peter M. Spa2p functions as a scaffold-like protein to recruit the Mpk1p MAP kinase module to sites of polarized growth. Current Biology, 2002, **12**(19): 1698–1703

[26] Brent Roger. Physiology and genetic regulation of cellular signal transmission. ICSB talk, 2007

[27] Bashor C J, Helman N C, Yan S, Lim W A. Using engineered scaffold interactions to reshape MAP kinase pathway signaling dynamics. Science, 2008, **319**(5869): 1539–1543